YTUP

Journal of Thermal Engineering
https://jten.yildiz.edu.tr/
https://doi.org/10.47481/jten.0004

RESEARCH ARTICLE

Component-based exergy modeling of three spool turboprop engine depending on the flight conditions

Onur Yuksel[1], Hakan Aygun[2,*]

[1]Graduate School of Natural and Applied Sciences, Firat University, Elazig, 23119, Türkiye
[2]Department of Aircraft Airframe and Powerplant, Firat University, Elazig, 23119, Türkiye

Abstract

Aero gas turbine engines, given their key role in aviation, have parameters that depend on flight conditions, and those parameters are extensively modeled using several approaches. Recently, energy and exergy metrics have revealed the engine's characteristics. In this study, flight-condition-based efficiency modeling is performed for the PW127-E turboprop engine and its components as employed in regional aircraft, thereby facilitating prediction of efficient operating points. Before exergetic analysis, thermodynamic data are obtained from real parametric cycle analyses for each component. Using regression analysis, energy and exergy parameters were modeled using cycle data across Mach numbers ranging from 0 to 0.6 and altitudes ranging from 0 to 6 km. Accordingly, the exergy efficiency of the combustor ranges from 71.37% to 74.37%, whereas that of the power turbine ranges from 95.46% to 96.27%. However, the exergy-destruction values for those ranges were between 1508 kW and 3121 kW and between 44.66 kW and 113.02 kW, respectively. On the other hand, R2 value of combustor exergy efficiency is computed as 0.9301 at linear model and 0.9997 at quadratic model whereas that of exergy efficiency of power turbine is measured as 0.9871 and 1, respectively. The results indicate that the exergetic parameters of components, when modeled as a function of flight conditions, exhibit a distinct pattern. Some components demonstrate nearly linear behavior, whereas others conform to a quadratic model. Due to the low model error in exergy, this study contributed significantly to the prediction of the exergetic parameters of components under flight conditions.

Keywords: Turboprop engine, exergy, modeling, flight condition

Cite this article as: Yuksel, O., & Aygun, H. (2026). Component-based exergy modeling of three spool turboprop engine depending on the flight conditions. Journal of Thermal Engineering, 12(3), 2–14. https://doi.org/10.47481/jten.0004

1. Introduction

Aircraft gas-turbine engines are designed to be relatively reliable despite their sophisticated systems. Therefore, these engines have attracted remarkable attention in different fields, which leads to special focusing on each of their systems [1]. Turboprop engines have, in particular, powered regional aircraft, a growing sector, because of their promising advantages, such as efficiency. Due to the importance of efficiency and its challenging role, scientists focus on increasing efficiency in every area of industry [2]. Moreover, gas turbine engines are affected by several factors, such as environmental impacts and the need for aircraft renewal. Especially, environmental issues have been dealt with by international associations such as ICAO, ATAG and IATA [3]. Since these have set several goals to mitigate the effects of global warming, the aviation sector could face challenges implementing these goals with existing technologies. According to Paris Aggrement, temperature rise is restricted by 1.5 $^{\circ}$C compared with pre-industrial years [4]. Therefore, substantial effort is required of all states and stakeholders to maintain the established goals. The aviation sector's steady growth has resulted in negative consequences, including increased emissions and noise pollution. In other words, it accounts for 2.1% of human-induced CO_2 emissions. When considering emissions worldwide, 914 million tonnes of CO_2 were produced in 2019 due to performed flights [5]. To tackle this concern, three pillars such as alternative fuels, operational measures and implementation of new technologies involving fully electrical aircraft and blended wing body are explicitly expressed in the literature [6] When it comes to greenhouse gases, CO_2 and H_2O are two main emissions, which are produced 3.16 kg and 1.23 kg per unit fuel of 1 kg, respective-

*Corresponding Author
E-mail Adress: haygun@firat.edu.tr

Submitted: 28 December 2025; **Accepted:** 17 January 2026

This paper was recommended for publication in revised form by Editorin-Chief Ahmet Selim Dalkılıç

Published by Yıldız Technical University, İstanbul, Türkiye

ly. Of which, CO_2 resides a long time in the atmosphere [7]. When considering the open literature about thermal modeling and optimization of several systems, there are many studies [8, 9]. This study examines turboprop engines used in aircraft, particularly regional ones. In this context, Kim et al. [10] aimed to determine the most effective method for updating the thermodynamic cycle model of a turboprop engine based on measurement data. A performance-adaptation approach was applied to improve the accuracy of the model, and three methods (Newton-Raphson + RCF, GA + RCF, and GA) were compared. According to the results, all methods achieved higher accuracy than the existing model, and the Newton-Raphson and RCF-based approaches showed the highest accuracy and lowest computational cost. Using this method, the maximum relative errors for fuel mass flow rate, compressor outlet pressure, and exhaust gas temperature were found to be 4.29%, 1.36%, and 3.49%, respectively.

Nicolosi et al. [3] investigated the design of a modern high-capacity turboprop aircraft with lower environmental impact compared to regional jets used for short and medium-range flights. Multidisciplinary optimization of three architectural configurations determined that a three-lifting-surface configuration for a 1600-NM range provided approximately 17.24% fuel savings. Compared with a new regional jet model developed under the same design requirements and with a 130-seat capacity, the turboprop configuration maintained its environmental advantage despite a decrease in block fuel savings from 7.24% to 5.96%. Kayaalp and Metlek [11] estimated exhaust emission indices based on air-fuel ratio, shaft speed, and fuel flow in the T56-A-15 turboprop engine. The performance of the model was evaluated using mean squared error (MSE), normalized mean squared error (NMSE), and mean absolute error (MAE). The MAE values for CO, CO_2, UHC, and NO_2 were 0.1473, 0.0442, 0.0369, and 0.0028, respectively. As a result, the model demonstrated high accuracy, yielding error values of 0.0266 for emission data and 7.6165×10^{-10} for combustion efficiency. Furthermore, Jakubowski and Jaklinski [12] constructed a computational model of a free power turbine engine within the MATLAB R2024b environment to evaluate engine performance. The model was developed to couple the engine geometry (determined at the design point) with variations in main-component performance by accounting for changes in operating conditions, such as rotor speed and environmental factors. The model, validated with data obtained from the PZL-3W engine, produced results showing strong agreement with experimental and literature data, demonstrating that engine performance could be reliably simulated. Kim et al. [13] developed a performance adaptation method to improve the prediction accuracy of a turboprop engine model based on flight condition measurement data. In this method, the efficiencies of the high-pressure compressor (HPC) and the power turbine (PT), the corrected mass flow rate, the HPC outlet pressure, and the high-pressure turbine (HPT) outlet temperature were adjusted using adaptation factors. The comparisons across ten operating points showed that the updated engine model significantly reduced the error relative to the measurement data collected under flight conditions. Lastly, Sharfabadi et al. [14] established a thermodynamic model of a turboprop engine and examined the performance relationships of components under on-design and off-design operating conditions. Performance curves for different turbine inlet temperatures, altitudes, and Mach numbers were compared and validated using GasTurb software. According to the results, a 10% increase in combustion-chamber pressure loss increases specific fuel consumption by 14%, whereas a 10% decrease in combustion efficiency increases specific fuel consumption by 13% and reduces engine power by 17.5%.

2. Exergetic studies related to turboprop engines

Aydin et al. [15] examined exergetic sustainability indicators for a turboprop engine in eight different flight phases. The results showed that the maximum exergy efficiency was 29.2%, the minimum waste exergy ratio was 70.8%, and the highest exergetic sustainability index was 0.41. During the taxi and landing phases, the exergy efficiency and exergetic sustainability index reached their lowest values, 20.6% and 0.26, respectively. Sahu and Choudhary [16] analyzed a cooled gas turbine-based turboprop engine from exergetic and exergoeconomic perspectives, examining the irreversibilities and inefficiencies in all engine components. As a result, the energetic and exergetic efficiencies of the air-cooled turboprop engine were 28.6% and 27.6%, respectively. Component-based exergetic efficiencies were 92.5% for the compressor, 76.8% for the combustion chamber, 92.2% for the gas turbine, 95.4% for the power turbine, 98% for the reduction gearbox, and 99% for the exhaust diffuser. Balli [17] presented exergetic and sustainability analyses of a medium-scale turboprop engine (m-TPE) utilized in Unmanned Aerial Vehicles (UAV). The exergy efficiency of the overall engine was calculated to be 17.24%. When examining component-based exergy efficiencies, the compressor reached 87.21%; the combustor reached 52.51%; the gas-generator turbine reached 98.53%; the power turbine reached 97.40%; and the exhaust duct reached 94.29%. Atilgan and Turan [18] achieved calculation of the dynamic exergy parameters for the compressor, combustion chamber, gas generator turbine, and power turbine by utilizing measured engine parameters, and based the exergoeconomic assessment on these results. According to the results, the exergy efficiency of the compressor remained approximately constant across all torque settings, with values of 0.85 at 240 Nm and 0.84 at other torque settings. Moreover, in the combustor the values were 0.76 at 240 Nm, 0.79 at 350 Nm, 0.81 at 485 Nm, and 0.82 for the remaining torques. The exergy efficiency of the gas-generator turbine varied between 0.92 and 0.97; that of the power turbine varied between 0.90 and 0.94; and that of the whole turboprop engine increased from 0.21 to 0.29 as torque increased from 240 Nm to 630 Nm. Dinc and Gharbia [19] computed main performance parameters of a turboprop engine such as exergy efficiency, shaft power, specific fuel consumption, fuel flow rate, and thermal efficiency within the range of 0–14 km altitude and Mach 0–0.6 speed. According to the study, the turboprop engine's exergy efficiency ranged from 23% to 33%, while its thermal efficiency ranged from 25% to 35%. Dursun et al. [20] measured performance and thermodynamic parameters of a conceptual turboprop engine (C-TPE) at fifty

different power settings and predicted these outputs by employing ANN and LSTM methods. Fuel flow rate, air mass flow rate, exhaust velocity, compressor pressure ratio, turbine outlet temperature, and revolutions per minute were used as inputs; net thrust, SFC, overall efficiency, exergy efficiency, and environmental impact factor were modeled as outputs. According to the results, the exergy efficiency remained in the range of 23.93%–26.2%. In exergy-efficiency modeling, ANN achieved an R^2 of 0.956493, whereas LSTM achieved an R^2 of 0.999061. Baklacioglu et al. [21] presented a deep artificial neural network (ANN) approach supported by a genetic algorithm (GA) to predict the relative exergy destruction of turboprop engine components. Increasing the number of hidden layers and appropriately selecting network weights significantly improved prediction accuracy compared to models with fewer layers. The ANN–GA hybrid structure further enhanced the accuracy (R) to values between 0.998929 and 0.999966. Kirmizi et al. [22] examined the performance and energy analyses of a turboprop engine operating at altitude of 6.7 km and Mach 0.59, considering design variables such as TIT (1200–1400 K), CPR (16–20), and propeller efficiency (PE = 0.7–0.98). Overall, efficiency increased as PE increased (from 21% to approximately 40%) and as TIT increased (from 26.3% to 28.12%), but decreased as CPR increased (from 27.6% to 23.5%). In multiple regression analysis, linear modeling yielded an R^2 of 0.97 for SFC and total efficiency; second-order modeling increased the R^2 to more than 0.99, and even linear approaches in models including PE resulted in an R^2 of 0.99. Lastly, Onur and Aygun [23] examined the performance parameters (SFC, thrust, thermal, and overall efficiency) of a turboprop engine for both ideal and actual conditions across altitudes of 0-9 km and Mach numbers of 0.3-0.6, and for design parameters (overall pressure ratio and turbine inlet temperature) ranging between 12-15 and 1200-1400 K, respectively. This study differs from the present study with respect to input variables, examined parameters, and methods.

A literature review reveals exergetic studies of various turboprop engines conducted at the design point, across different flight phases, and considering different design variables. The lack of component-level modeling of exergetic parameters is the main motivation for this study. The originality of this study lies in the modeling of the exergy efficiency and exergy destruction of the PW127-E engine and its components across flight conditions. To summarize the analyses presented here, we performed (i) component-level exergy analysis; (ii) analysis of the effect of Mach number and altitude on exergy parameters; and (iii) regression analysis of component exergy efficiencies using the obtained dataset.

3. System description

PW100-series turboprop engines power regional aircraft that seat 30–90 passengers and have ranges of up to 750 miles. The engines offer high reliability, efficiency, and long life, and their versatility allows them to be used in a variety of applications [24]. These consist of a three-shaft turbomachinery with a free turbine and a reduction gearbox [25]. In this study, the analyses are performed on a turboprop engine similar to the PW127-E. Figure 1 shows a two-dimensional cross-sectional view of the PW127 turboprop engine. Moreover, Table 1 presents the key features of the related turboprop engine.

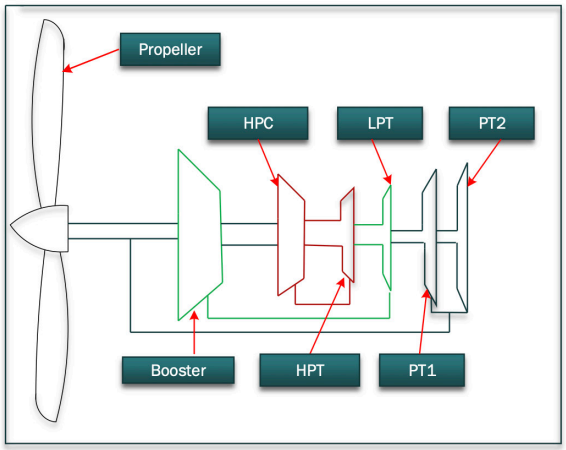

Figure 1. Representative drawing of typical PW127 engine

Table 1. Specifications of turboprop engine [23, 26]

Parameters	Nominal values
Ambient temperature (K)	288.15
Ambient pressure (kPa)	101.325
Air mass flow ($\dot{m}_a$) (kg/s)	8.5
Overall pressure ratio	15.7
Turbine inlet temperature (K)	1260
Power (kW)	1790
Overall weight (kg)	480.8

4. Methodology

In this study, the inlet and outlet pressures and temperatures of the components, the air mass flow rate, and the fuel flow rate are computed using parametric cycle analysis. Then, an exergy analysis is carried out for each component. Moreover, regression analysis was conducted to model component exergetic parameters based on the obtained dataset. Several fundamental assumptions were adopted when performing exergy analysis: (i) steady-state conditions were assumed for the operation of the turboprop engine; (ii) both air and combustion products were modeled as ideal gases; (iii) complete combustion was assumed; and(iv)variations in kinetic and potential exergy were omitted.

4.1. Exergetic relations

The phsyical exergy (ψ) for working fluid is measured as follows [17, 27, 28]:

$$\psi = (h - h_0) - T_0(s - s_0) \quad (1)$$

where h and s represent enthalpy and entropy, respectively.

Assuming constant specific heat, the physical exergy of air and gas can be calculated using Eq. 2.

$$\dot{E}x^{PH} = \dot{m}_a\left[c_p\left(T - T_0 - T_0 \ln\frac{T}{T_0}\right) + RT_0 \ln\frac{P}{P_0}\right] \quad (2)$$

where $\dot{m}_a$, T and P denote air mass flow, temperature and pressure, in turn.

For any turbomachinery component, the exergy change could be represented as follows [29].

$$\Delta\psi = \psi_2 - \psi_1 = (h_2 - h_1) - T_0(s_2 - s_1) \quad (3)$$

Similar to energy, exergy can be transferred between a system and its surroundings through mass, work, and heat interactions. To formulate the exergy balance, all of these modes of transfer must be taken into account within a defined control volume. For steady-state conditions, the exergy balance can be expressed as follows.[27, 30, 31]:

$$\sum\left(1 - \frac{T_0}{T_k}\right)\dot{Q}_k - \dot{W} + \sum_{in}\dot{m}\dot{\psi} - \sum_{out}\dot{m}\psi - \dot{X}_{dest} = \frac{dX_{cv}}{dt} \quad (4)$$

4.2. Application of exergy analysis to components of turboprop engine

Calculating exergy destruction and exergy efficiency requires determining the actual and ideal work(exergy)of the components. Formulas for these parameters are presented for each component. Figure 2 depicts the main components of a turboprop engine.

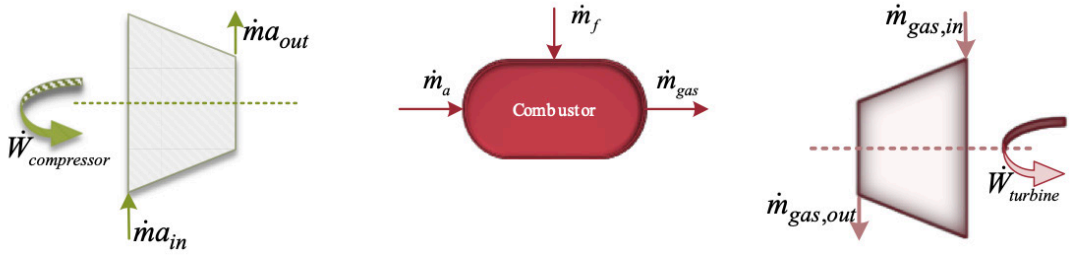

Figure 2. Cross section of turbomachinery and combustor components

4.3. For booster and high pressure compressor

In this section, the actual work, exergy destruction, and exergy efficiency formulas are provided for the booster and HPC [28, 32, 33].

$$\dot{W}_{comp} = \dot{m}_{out}(h_{out} - h_{in}) \quad (5)$$

$$\dot{E}x_{dest,comp} = \dot{W}_{comp} - (\dot{E}x_{out,comp} - \dot{E}x_{in,comp}) \quad (6)$$

$$\eta_{ex,comp} = 1 - \frac{\dot{E}x_{dest,comp}}{\dot{W}_{comp}} \quad (7)$$

where $\dot{W}_{comp}$ represents real work regarding compressor whereas

$\dot{E}x_{dest,comp}$ and $\eta_{ex,comp}$ denote exergy destruction and exergy efficiency, respectively.

4.3. Combustor

In this section, the fuel exergy, exergy destruction, and exergy efficiency formulas are provided for combustor.

$$\dot{E}x_{in,fuel} = \dot{m}_f Q_{LHV}\,\xi \quad (8)$$

$$\dot{E}x_{dest,comb} = \dot{E}x_{in,comb} + \dot{E}x_{in,fuel} - \dot{E}x_{out,comb} \quad (9)$$

$$\eta_{ex,comb} = 1 - \frac{\dot{E}x_{dest,comb}}{\dot{E}x_{in,comb} + \dot{E}x_{in,fuel}} \quad (10)$$

4.4. Turbine units

In this section, the actual work, exergy destruction, and exergy efficiency formulas are provided for the HPT, IPT and PT units.

$$\dot{W}_{turb} = \dot{m}_{out}(h_{in} - h_{out}) \quad (11)$$

$$\dot{E}x_{dest,turb} = (\dot{E}x_{in,turb} - \dot{E}x_{out,turb}) - \dot{W}_{turb} \quad (12)$$

$$\eta_{ex,turb} = 1 - \frac{\dot{E}x_{dest,turb}}{(\dot{E}x_{in,turb} - \dot{E}x_{out,turb})} \quad (13)$$

where $\dot{W}_{turb}$ represents real work regarding compressor whereas $\dot{E}x_{dest,turb}$ and $\eta_{ex,turb}$ denote exergy destruction and exergy efficiency, respectively.

4.5. Regression analysis

It is a method for determining the relationship between a variable and other variables. It typically examines the relationship between the dependent variable Y and the X variables, often called independent or explanatory variables. The dependent variable has a numerical value, whereas the independent variables can be numerical, binary, or multi-categorical [34]. The objectives and methods of simple linear regression can be extended to multiple linear regression models to include additional predictor variables. This study examines the relationships between the dependent variables (exergy destruction and exergy efficiency) and the independent variables (Mach and altitude). In this model, the coefficients are determined to minimize the sum of squared residuals values, as in the simple linear regression method [35]. Generally, the dependant variable in multiple linear regression can be related to n regressors, x_1, x_2, … and x_n [36].

$$y_i = \beta_0 + \beta_1 x_i + \epsilon_i \tag{14}$$

where ϵ_i is random error component and β_0 and β_1 are unknown constants. To forecast β_0 and β_1, technique of the least squares is employed [36].

$$S(\beta_0, \beta_1) = \sum_i^n (y_i - \beta_0 - \beta_1 x_i)^2 = (\epsilon_i)^2 \tag{15}$$

In this study, modeling performance is determined by sum squared error (SSE), root mean square error (RMSE) and coefficient of determination (R^2), respectively.

$$SSE = \sum_i^n (y_i - \hat{y}_i)^2 \tag{16}$$

$$RMSE = \sqrt{\frac{1}{n}} \tag{17}$$

$$R^2 = 1 - \frac{\sum_{i=1}^n (y_i - \hat{y}_i)^2}{\sum_{i=1}^n (y_i - \bar{y}_i)^2} \tag{18}$$

where y_i, $\hat{y}_i$ and $\bar{y}_i$ denote real, predicted and average of values, respectively.

Figure 3 shows the steps for modeling component exergy parameters. Accordingly, Mach and altitude are specified. Then the thermodynamic parameters (temperature and pressure) are computed. Based on this, an exergy analysis was performed, and regression analysis was applied to six components using the obtained dataset.

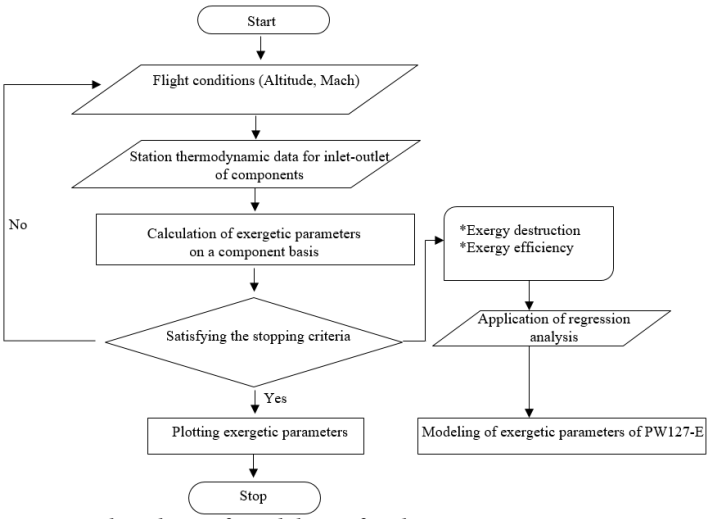

Figure 3. Flowchart of modeling of turboprop engine components

5. Results and discussion

This study analyzes how exergy destruction and exergy efficiency of the six main components of a turboprop engine (booster, high-pressure compressor, combustor, high-pressure turbine, intermediate turbine, and power turbine) vary with altitude and Mach number. Additionally, the results, based on the obtained data, of linear and quadratic regression analyses of the components are presented.

Figure 4a shows the variation in exergy destruction associated with the booster at different Mach numbers and altitudes. Accordingly, it varies between 32.908 kW and 93.794 kW for both flight variables. When Mach is held constant at 0.3, exergy destruction decreases from 80.28 kW to 34.72 kW, corresponding to a 56.75% reduction at elevated altitude. Furthermore, at a constant altitude of 3 km, it increases from 50.78 kW to 62.61 kW, representing a 23.29% increase. When it comes to modeling findings, R^2 of the booster exergy efficiency is measured as 0.979 in linear modeling whereas it is enhanced to 0.9994 in quadratic modeling.

Figure 4b illustrates the variation in the exergy destruction of the HPC component across flight conditions. Exergy destruction is observed between 66.803 kW and 191.128 kW across both variable ranges. Accordingly, at a constant speed of Mach 0.3, exergy destruction decreases from 163.44 kW at 0 km altitude to 70.5 kW at 6 km. However, at a constant altitude of 3 km, exergy destruction increases from 103.28 kW to 127.45 kW. Finally, for HPC exergy destruction, R^2 is found to be 0.9828 with the linear model, while it improves to 0.9995 with the quadratic model.

Figure 4c shows the trend in exergy destruction in the combustion chamber as a function of altitude and Mach number. Accordingly, this parameter was determined to be between 1508.379 kW and 3121.8 kW. When the Mach number is held constant at 0.3, the exergy destruction decreases from 2870.59 kW to 1562.12 kW with

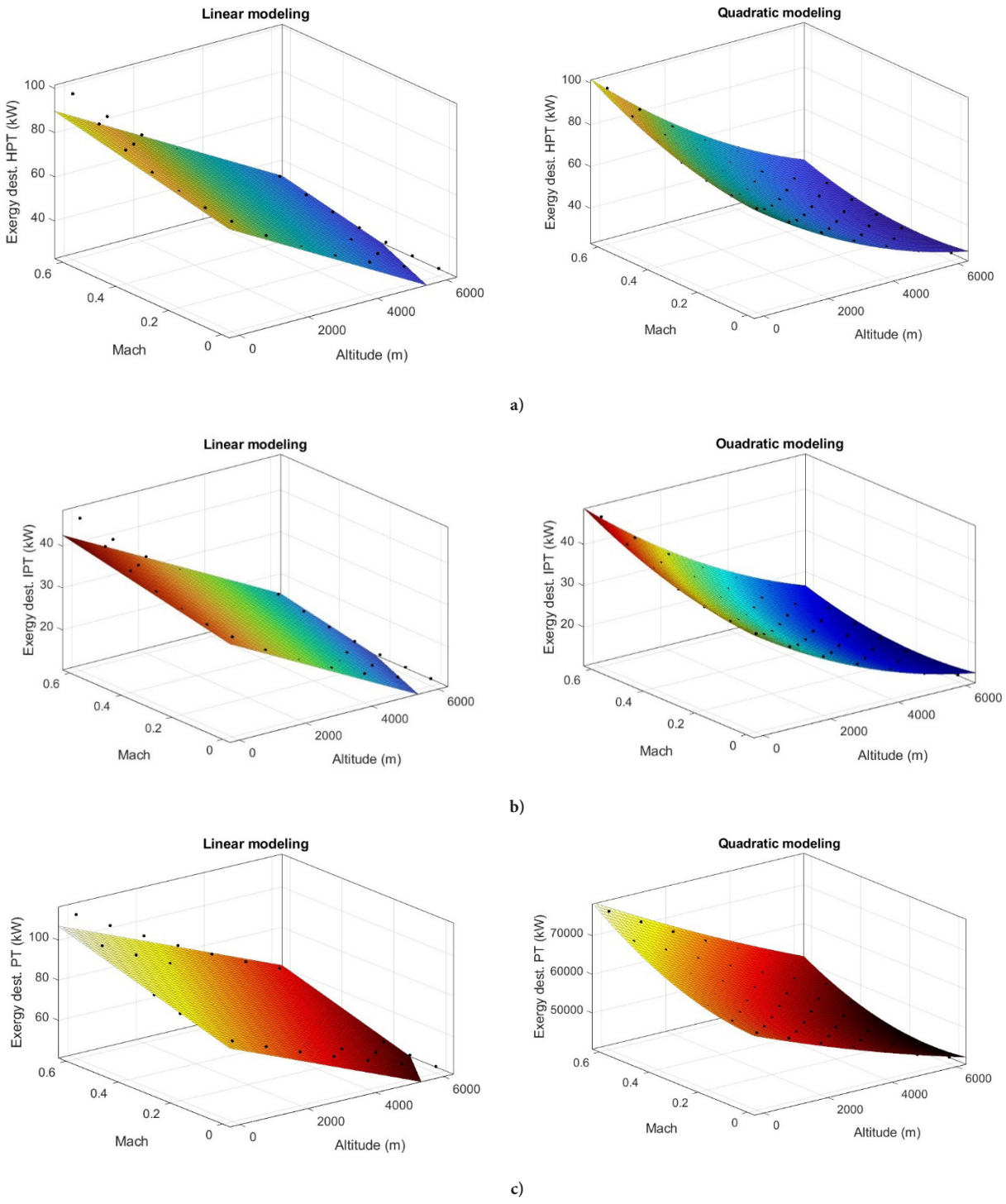

Figure 4. Exergy destruction and modeling of booster, HPC and combustor units

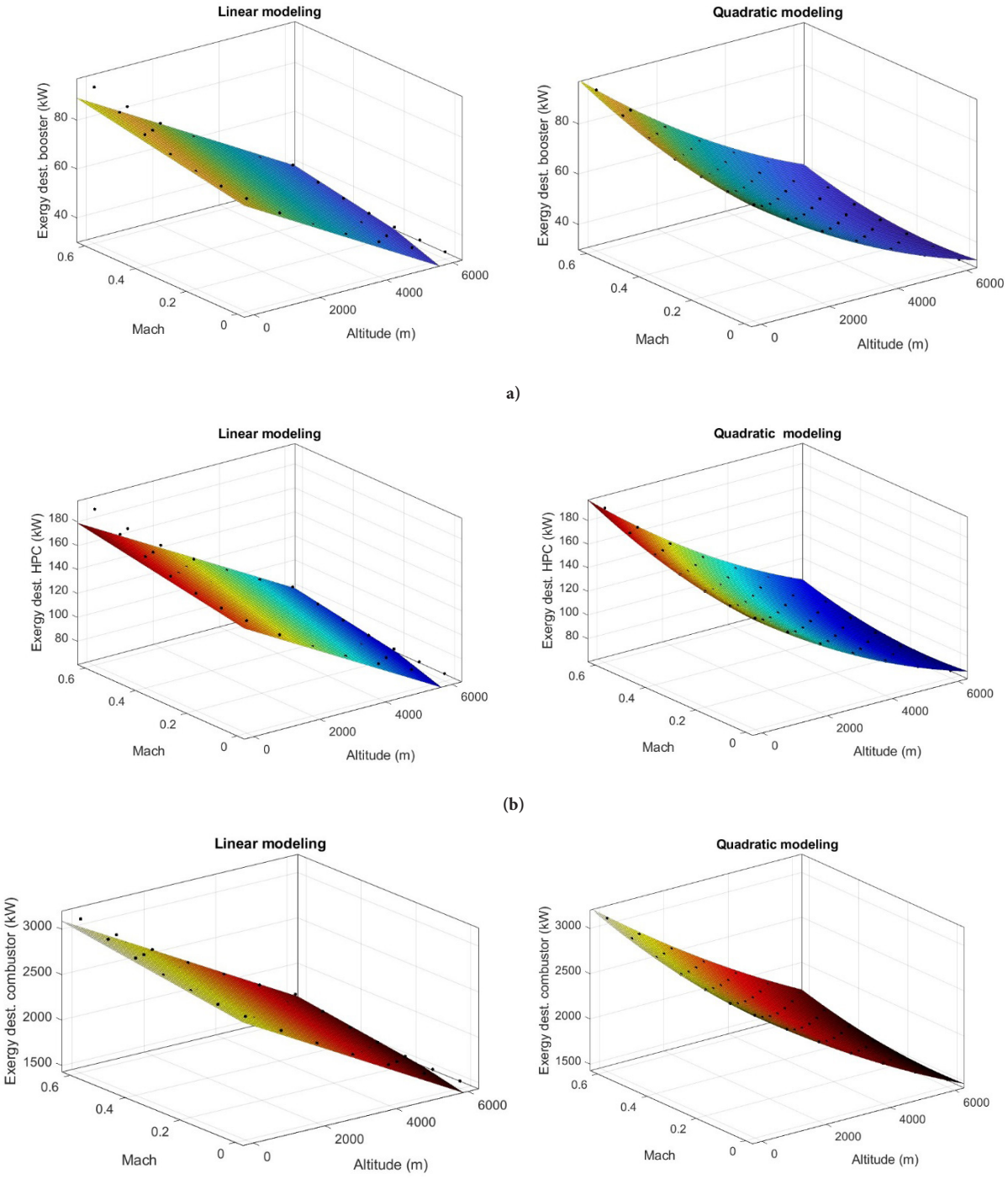

Figure 5. Exergy destruction and modeling of turbine units

increasing altitude. Moreover, at an altitude of 3 km, the exergy destruction of the combustor increases from 2083.84 kW to 2355.66 kW. On the other hand, according to the modeling findings, while the magnitude of R^2 is computed as 0.9927 in the linear model, it is improved to 0.9999 in the quadratic model.

Table 2 presents the error values and R^2 values related to the modeling success of exergy destruction for the booster, HPC, and combustion chamber. When the polynomial model changes from linear to second-degree form, improvement is observed. Namely, the RMSE value for the booster decreases from 2371 to 393.1, whereas for the HPC it drops from 4476 to 720.4. Finally, the RMSE for the combustion chamber improves from $3.988*10^4$ to $0.4066*10^4$.

Table 2. Model errors regarding exergy destruction of booster, HPC and combustor

Exergy destruction	Linear modeling			Quadratic modeling		
	SSE	RMSE	R^2	SSE	RMSE	R^2
Booster	$2.587*10^8$	2371	0.979	$6.645*10^6$	393.1	0.9994
HPC	$9.215*10^8$	4476	0.9828	$2.231*10^7$	720.4	0.9995
Combustor	$7.315*10^{10}$	$3.988*10^4$	0.9927	$7.108*10^8$	$0.4066*10^4$	0.9999

Figure 5a shows the variation of exergy destruction in the high-pressure turbine (HPT) as a function of Mach number and altitude. In this regard, it ranges between 26.51 kW and 97.89 kW for both flight variables. At Mach 0.3, exergy destruction decreases from 78.66 kW to 28.57 kW, representing a 63.67% reduction attributable to increased altitude. Furthermore, at a constant altitude of 3 km, it increases from 44.77 kW to 60.02 kW, representing a 34.06% increase. When it comes to modeling findings, R^2 of the booster exergy destruction is measured as 0.9679 in linear modeling whereas it enhances to 0.9988 in quadratic modeling.

Figure 5b depicts the variation in exergy destruction of the intermediate power turbine (IPT) under different flight conditions. Exergy destruction ranged from 12.20 kW to 46.84 kW across the two variable ranges. Accordingly, at a constant Mach number of 0.3, exergy destruction decreases from 37.23 kW to 13.18 kW as altitude increases from 0 to 6 km. Furthermore, at a constant altitude of 3 km, exergy destruction rises from 20.85 kW to 28.28 kW. Finally, for HPC exergy destruction, R^2 is found to be 0.9652 with the linear model, while it increased to 0.9987 with the quadratic model.

Figure 5c shows the trend in exergy destruction in the power turbine (PT) with respect to altitude and Mach number. In this context, this parameter is observed to lie between 44.66 kW and 113.02 kW. At a constant Mach of 0.3, the exergy destruction decreases from 88.72 kW to 48.69 kW as altitude increases. Moreover, at an altitude of 3 km, an increase in the exergy destruction of the power turbine, from 61.62 kW to 85.64 kW, was observed. On the other hand, according to the modeling findings, whereas the R^2 value is calculated as 0.9650 in the linear model, it improves to 0.9999 in the quadratic model.

Table 3 illustrates the error values and R^2 values related to the modeling success of exergy destruction for the HPT, IPT, and PT. As can be seen in table 3, the RMSE value for the HPT decreases from 3389 to 663.6, whereas for the IPT it drops from 1701 to 345.1. Finally, the RMSE for the PT decreased from 3159 to 541.5.

In the following section, the results are presented in Figures 6 and 7, along with exergy efficiency and its modeling. Figure 6a shows the variation of booster exergy efficiency as a function of Mach number and altitude. Accordingly, it varies between 93.131% and 93.599% across both flight variables. When Mach is kept constant at 0.3, exergy destruction increases slightly, from 93.25% to 93.26%, at elevated altitude. Furthermore, at a constant altitude of 3 km, it increases from 93.13% to 93.59%, an increase of 0.46%. When it comes to modeling findings, R^2 of the booster exergy efficiency is determined as 0.9317 in linear modeling whereas it enhances to 0.9999 in quadratic modeling.

Figure 6b illustrates the variation in the exergy efficiency of the HPC component as a function of flight conditions. Exergy efficiency ranges between 93.531% and 93.991% across both variable ranges. Accordingly, at a constant speed of Mach 0.3, exergy destruction increased from 93.639% to 93.689% as altitude increased from 0 to 6 km. However, at an altitude of 3 km, exergy destruction increases from 93.556% to 93.966%. Finally, for HPC exergy destruction, R^2 is found to be 0.9326 with the linear model, whereas it enhances to 0.9999 with the quadratic model.

Table 3. Model errors regarding exergy destruction of turbine units

Exergy destruction	Linear modeling			Quadratic modeling		
	SSE	RMSE	R^2	SSE	RMSE	R^2
HPT	$5.284*10^8$	3389	0.9679	$1.893*10^7$	663.6	0.9988
IPT	$1.331*10^8$	1701	0.9652	$5.121*10^6$	345.1	0.9987
PT	$4.589*10^8$	3159	0.9650	$1.261**10^7$	541.5	0.9999

Figure 6c shows the variation of exergy efficiency of the combustion chamber with altitude and Mach number. This parameter ranges from 71.378% to 74.372%. At Mach 0.3, the exergy efficiency decreases from 72.668% to 71.851% as altitude increases. At an altitude of 3 km, the combustor's exergy efficiency increases from 71.64% to 73.74%. On the other hand, according to the modeling findings, while the R^2 value is calculated as 0.9301 in the linear model, it improves to 0.9997 in the quadratic model.

Table 4 depicts the error values and R^2 values related to the modeling success of exergy efficiency for the booster, HPC, and combustion chamber. As can be understood, the RMSE value for the booster decreases from $4.285*10^{-4}$ to $1.86*10^{-5}$, whereas for the HPC it diminishes from $3.851*10^{-4}$ to $1.653*10^{-5}$. Finally, the RMSE for the combustion chamber improves from $2.139*10^{-3}$ to $1.41*10^{-4}$.

Table 4. Model errors regarding exergy efficiency of booster, HPC and combustor

Exergy efficiency	Linear modeling	Quadratic modeling

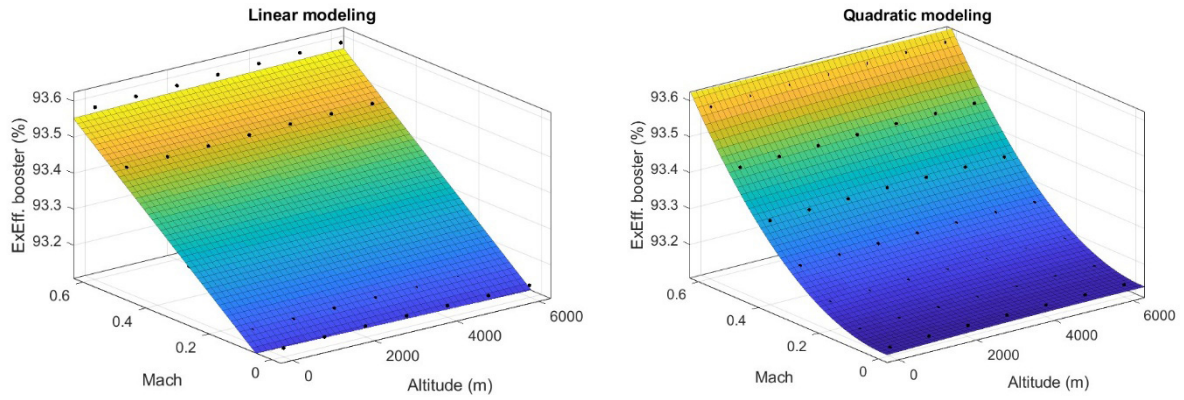

a)

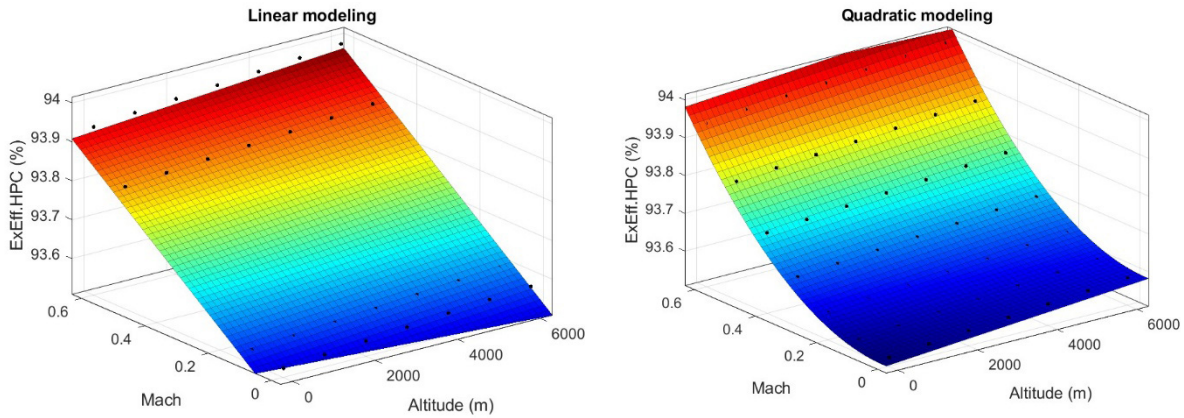

b)

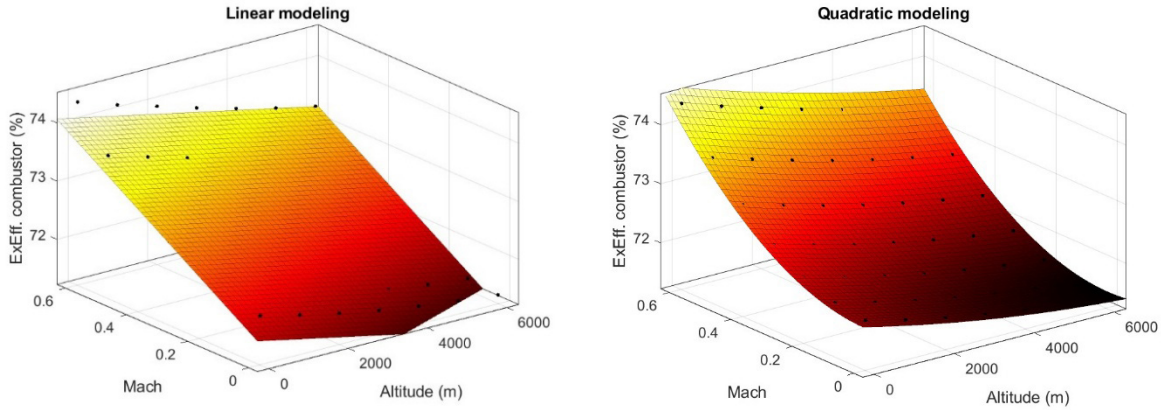

c)

Figure 6. Exergy efficiency and modeling of booster, HPC and combustor units

	SSE	RMSE	R^2	SSE	RMSE	R^2
Booster	$8.445*10^{-6}$	0.0004285	0.9317	$1.488*10^{-8}$	$1.86*10^{-5}$	0.9999
HPC	$6.823*10^{-6}$	0.0003851	0.9326	$1.175*10^{-8}$	$1.653*10^{-5}$	0.9999
Combustor	0.0002105	0.002139	0.9301	$8.548*10^{-7}$	0.000141	0.9997

Figure 7. Exergy efficiency and modeling of turbine units

Figure 7a illustrates the variation in exergy efficiency of the HPT across different Mach numbers and altitudes. Accordingly, it varies between 97.048% and 97.563% for both flight variables. When Mach is held constant at 0.3, exergy efficiency increases from 97.087% to 97.554%, which corresponds to a 0.467 percentage-point increase due to an increase in altitude. Furthermore, at a constant altitude of 3 km, it decreases from 97.335% to 97.291%, corresponding to a 0.044% decrease. When it comes to modeling findings, R^2 of the booster exergy efficiency is measured as 0.9991 in linear modeling whereas it enhances to 1 in quadratic modeling.

Figure 7b illustrates the variation in the IPT unit's exergy efficiency under different flight conditions. Exergy efficiency ranged between 96.956% and 97.567% across both variable ranges. Moreover, at a constant speed of Mach 0.3, as altitude increases from 0 to 6 km, the

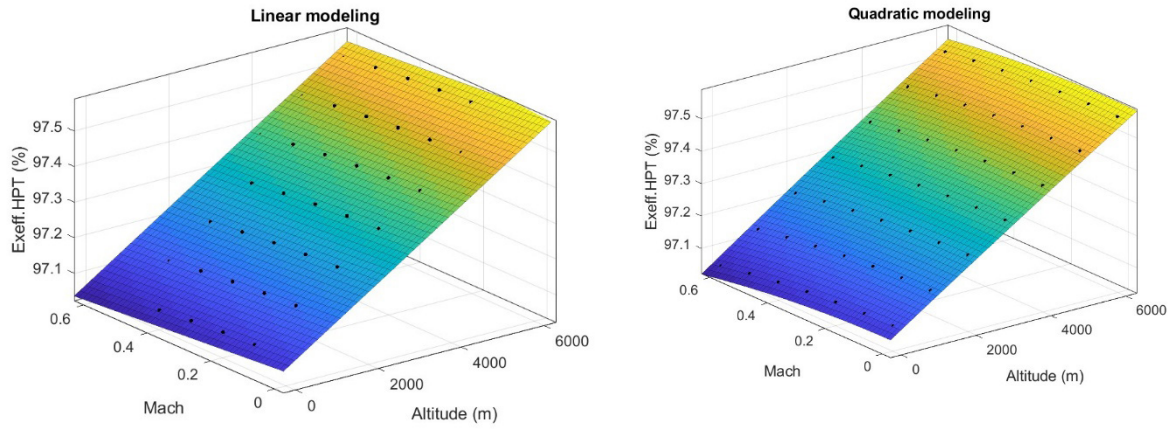

a)

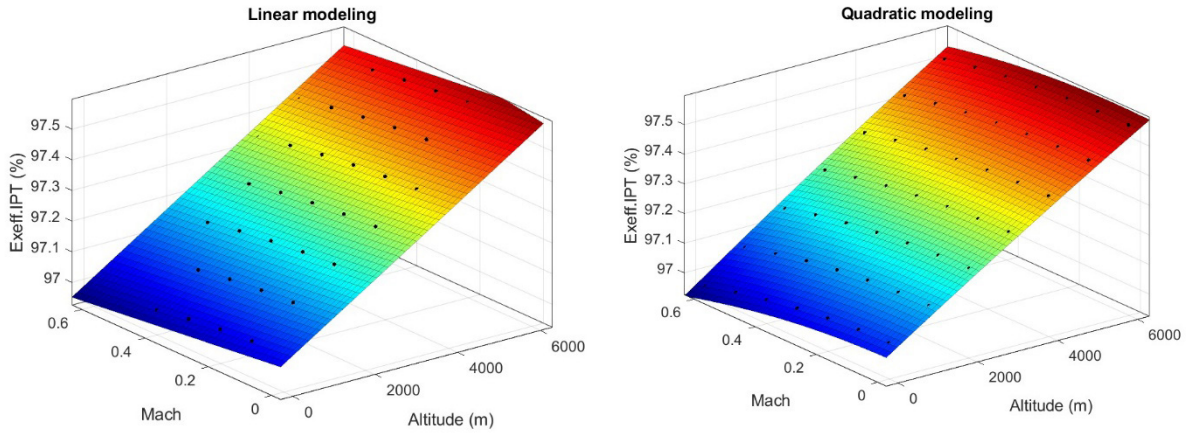

b)

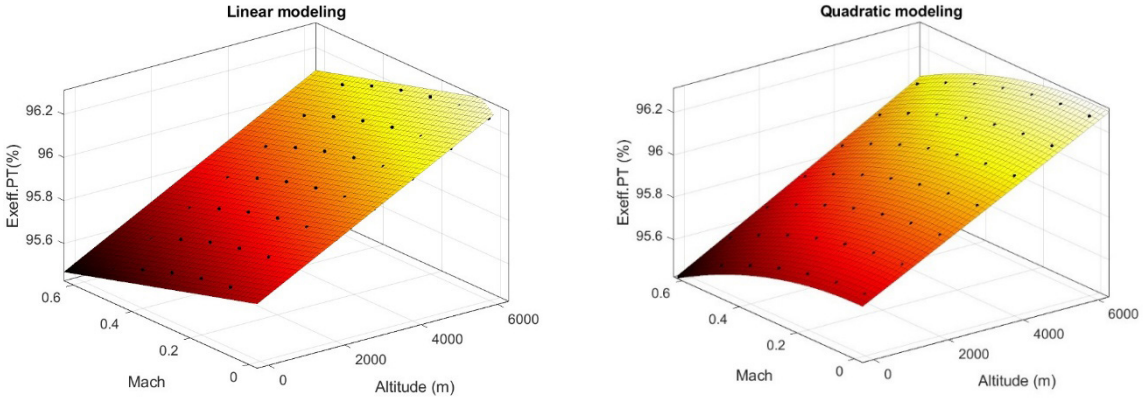

c)

exergy efficiency increases from 97.024% to 97.552%. At a constant altitude of 3 km, the exergy efficiency decreases from 97.313% to 97.242%. Finally, for IPT exergy efficiency, R^2 is found to be 0.9976 with the linear model, while it increased to 1 with the quadratic model.

Figure 7c shows the variation in the exergy efficiency of the PT with respect to altitude and Mach number. Accordingly, this parameter ranged between 95.465% and 96.273%. When the Mach number is held constant at 0.3, the exergy efficiency increases from 95.653% to 96.218% as altitude increases. At an altitude of 3 km, the exergy efficiency of PT decreases from 95.993% to 95.758%. On the other hand, according to the modeling findings, while the R^2 value is computed as 0.9876 in the linear model, it improves to 1 in the quadratic model.

Table 5. Model errors regarding exergy efficiency of turbine units

Exergy efficiency	**Linear modeling**			**Quadratic modeling**		
	SSE	RMSE	R^2	SSE	RMSE	R^2
HPT	$1.126*10^{-7}$	$4.948*10^{-5}$	0.9991	$1.117*10^{-9}$	$5.097*10^{-6}$	1
IPT	$3.698*10^{-7}$	$8.966*10^{-5}$	0.9976	$7.282*10^{-9}$	$1.301*10^{-5}$	1
PT	$2.58*10^{-6}$	0.0002368	0.9876	$4.896*10^{-9}$	$1.067*10^{-5}$	1

Table 5 tabulates the error values and R^2 values related to the modeling success of exergy efficiency for the HPT, IPT, and PT. As can be seen in table 5, the RMSE value for the HPT decreases from $4.948*10^{-5}$ to $5.097*10^{-6}$, whereas for the IPT it drops from $8.966*10^{-5}$ to $1.301*10^{-5}$. Finally, the RMSE for the PT improves from 2.36810^{-4} to $1.067*10^{-5}$.

Figure 8 depicts the variation in the overall exergy efficiency of the PW127-E engine across different Mach numbers and altitudes. Accordingly, it fluctuates between 26.46% and 33.08% across both flight variables. When Mach is kept constant at 0.3, exergy efficiency increases from 27.48% to 30.25%, which corresponds to an improvement of 2.77 percentage points attributable to elevated altitude. Furthermore, at a constant altitude of 3 km, it increases from 27.96% to 31.87%, representing a 3.91% increase. When it comes to modeling findings, R^2 of exergy efficiency of the whole engine is measured as 0.9483 in linear modeling whereas it enhances to 1 in quadratic modeling.

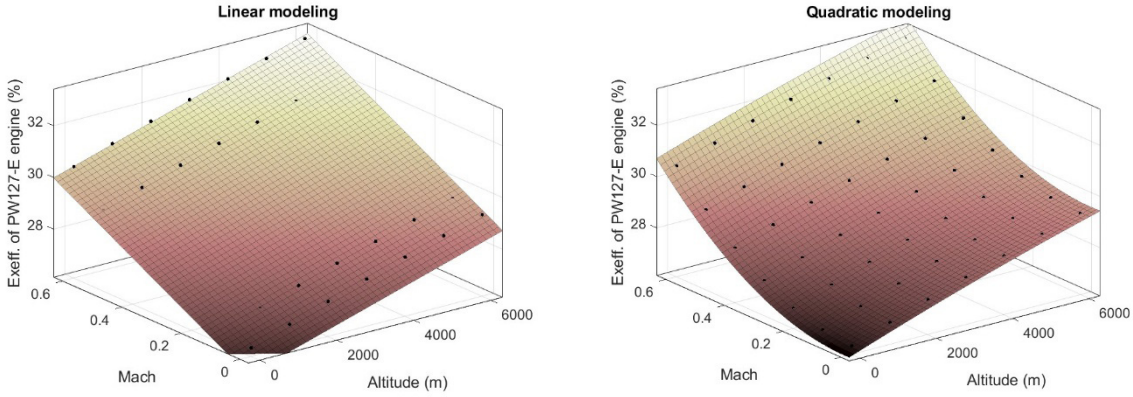

Figure 8. Exergy efficiency and modeling of overall turboprop engine

Table 6 presents comparative results from the current and previous studies. Accordingly, the exergy efficiency results obtained are consistent with those reported in the literature. In other words, while the exergy efficiency for the overall turboprop engine is found to be between approximately 26% and 33%, values in the literature range from approximately 20% to 33%. This difference can be explained by the characteristics of the engine under study and the types and ranges of the input parameters examined.

Table 6. Comparative results of exergy efficiency and R^2

Overall turboprop engine	Exergy efficiency (%)	R^2
Ref. [15]	20.6%-29.2%	NA
Ref. [18]	21%-29%	NA
Ref. [19]	23%–33%	NA
Ref. [20]	23.93%–26.2%	0.956493-0.999061
Present study	26.46%-33.08%	0.9483-1

Lastly, table 7 shows the error values and R^2 values related to the modeling success of exergy efficiency for overall engine of PW127-E turboprop engine. Accordingly, the RMSE value for the engine decreases from $3.836*10^{-3}$ to $9.151*10^{-5}$.

Table 7. Model errors regarding exergy efficiency of the overall engine

Exergy efficiency	Linear modeling			Quadratic modeling		
	SSE	RMSE	R^2	SSE	RMSE	R^2
PW127-E	0.0006768	0.003836	0.9483	$3.601*10^{-7}$	$9.151*10^{-5}$	1

6. Conclusion

Recently, studies of turboprop engines, a type of aircraft engine, have become increasingly prevalent. To the best of the authors' knowledge, this study is the first to perform exergy and regression analyses of PW127-E turboprop engine components under flight conditions. Specifically, temperature, pressure, and airflow for the components under each flight condition are obtained via parametric cycle analysis. Then, an exergy analysis is applied to six units of the turboprop engine. In this context, exergy destruction and exergy efficiency are calculated for each component. Modeling is performed on the obtained dataset using regression analysis. To summarize the analysis remarks,

- The effect of altitude on exergy destruction is found to be as significant as that of the Mach number. Exergy destruction varies approximately between 45% and 65% with changes in altitude and between approximately 13% and 38% with changes in Mach number.
- The exergy efficiency of the combustion chamber was observed to range between 71.378% and 74.372% depending on altitude and Mach number. This change corresponds to approximately 3%.
- Using the quadratic model significantly improves the modeling of exergy destruction in turbine units. R^2 increases from approximately 0.96 to over 0.99.

In the exergy efficiency model, the exergy efficiencies of the booster, high-pressure compressor, and combustor units from an R^2 of approximately 0.93 to an R^2 of over 0.99 owing to the quadratic model.

Lastly, the exergy efficiency of the overall turboprop engine varied between 26.46% and 33.08%, corresponding to a variation of 6.62%.

This study found that turboprop engine components can be modeled with a relatively low error rate. This analysis demonstrates that it can be applied to other aviation engine components. Modeling can optimize exergetic parameters under different flight conditions. In a future study, turboprop exergetic parameters could be predicted using machine learning algorithms for comparative evaluation. Based on this analysis, a multi-objective optimization of the turboprop engine's thermodynamic parameters with respect to flight conditions and design parameters can be performed.

Authorship contributions

Onur Yuksel: Writing—original draft preparation, conceptualization, and methodology. Hakan Aygun: Writing-Original draft preparation, Methodology, Editing, Reviewing and Supervision.

Data availability statement

The authors confirm that the data supporting the findings of this study are available within the article. Raw data supporting the findings of this study are available from the corresponding author upon reasonable request.

Conflict of interest

The author declared no potential conflicts of interest with respect to the research, authorship, or publication of this article.

Ethics

There are no ethical issues with the publication of this manuscript.

Statement on the use of artificial intelligence

Artificial intelligence was not used in the preparation of the article.

Nomenclature

ANN	Artificial neural network
CPR	Compressor pressure ratio
h	Enthalpy(kJ/kg)
HPC	High-pressure compressor
HPT	High-pressure turbine
IPT	Intermediate-pressure turbine
$\dot{m}$	Mass flow(kg/s)
MAE	Mean absolute error
P	Pressure(kPa)
PE	Propeller efficiency
PT	Power turbine
R^2	Coefficient of determination
RMSE	Root mean square error
s	Entropy
SSE	Sum squared error
TIT	Turbine inlet temperature
UAV	Unmanned aerial vehicle

Greek symbols

Ψ	Physical exergy
η	Efficiency
β	Constant

Subscripts

a	Air
f	Fuel
PH	Physical

References

[1] Liu L., Song X.,Zhou Z.(2022)"Aircraft engine remaining useful life estimation via a double attention-based data-driven architecture".Reliability Engineering & System Safety 221: 108330. https://doi.org/10.1016/j.ress.2022.108330.

[2] Panda S., Baag A.P., Pattnaik P.K., Baithalu R.,Mishra S.R.(2025)"Artificial neural network approach to simulate the impact of concentration in optimizing heat transfer rate on water-based hybrid nanofluid under slip conditions: A regression analysis".Numerical Heat Transfer, Part B: Fundamentals 86(7): 2301-2323. 10.1080/10407790.2024.2333944.

[3] Nicolosi F., Corcione S., Trifari V.,De Marco A.Design and Optimization of a Large Turboprop Aircraft. Aerospace 2021; 8(5). 10.3390/aerospace8050132.

[4] Zaporozhets O., Isaienko V.,Synylo K.(2020)"Trends on current and forecasted aircraft hybrid electric architectures and their impact on environment".Energy 211: 118814. https://doi.org/10.1016/j.energy.2020.118814.

[5] ATAG. 2023; Available from: https://atag.org/facts-figures.

[6] Abrantes I., Ferreira A.F., Silva A.,Costa M.(2021)"Sustainable aviation fuels and imminent technologies - CO2 emissions evolution towards 2050".Journal of Cleaner Production 313: 127937. https://doi.org/10.1016/j.jclepro.2021.127937.

[7] Sher F., Raore D., Klemeš J.J., Rafi-ul-Shan P.M., Khzouz M., Marintseva K.,Razmkhah O.(2021)"Unprecedented Impacts of Aviation Emissions on Global Environmental and Climate Change Scenario".Current Pollution Reports 7(4): 549-564. 10.1007/s40726-021-00206-3.

[8] Mishra S.R., Pattnaik P.K., Baithalu R., Ratha P.K.,Panda S.(2024)"Predicting heat transfer Performance in transient flow of CNT nanomaterials with thermal radiation past a heated spinning sphere using an artificial neural network: A machine learning approach".Partial Differential Equations in Applied Mathematics 12: 100936. https://doi.org/10.1016/j.padiff.2024.100936.

[9] Baithalu R.,Mishra S.R.(2025)"Response surface methodology in optimizing heat transfer rate for homogeneous–heterogeneous reactions with thermal radiation effect on the micropolar nanofluid".Numerical Heat Transfer, Part A: Applications 86(6): 1773-1792. 10.1080/10407782.2023.2282152.

[10] Kim S., Lee C.-R., Yang W.,Kim Y.(2024)"Suitability of performance adaptation methods for updating the thermodynamic cycle model of a turboprop engine".Applied Thermal Engineering 242: 122408. https://doi.org/10.1016/j.applthermaleng.2024.122408.

[11] Kayaalp K.,Metlek S.(2021)"Prediction of burning performance and emissions indexes of a turboprop motor with artificial neural network".Aircraft Engineering and Aerospace Technology 93(3): 394-409. 10.1108/AEAT-08-2020-0177.

[12] Jakubowski R.,Jakliński P.A Practical Approach to Modeling and Performance Analysis of a Turboshaft Engine Using Matlab. Applied Sciences 2024; 14(23). 10.3390/app142311373.

[13] Kim S., Kwon Y.-M., Chun Y., Lee C.-R., Yang W.,Kim Y. Sequential Performance Adaptation for a Turboprop Engine Model at Flight Condition. in Turbo Expo: Power for Land, Sea, and Air.(Year)of Conference.: American Society of Mechanical Engineers.

[14] Mazidi Sharfabadi M., Seraj A.,Kahd Narouei M.E.(2021)"A Turboprop Engine Modeling in the Design and Off-Design Conditions to Investigate the Effect of Combustion Chamber Defects on its Performance".Fluid Mechanics & Aerodynamics 10(1): 99-114.

[15] Aydın H., Turan Ö., Karakoç T.H.,Midilli A.(2013)"Exergo-sustainability indicators of a turboprop aircraft for the phases of a flight".Energy 58: 550-560. https://doi.org/10.1016/j.energy.2013.04.076.

[16] Sahu M.K.,Choudhary T., Exergoeconomic Analysis of air cooled turboprop engine: air craft application. 2017, SAE Technical Paper.

[17] Ballı Ö.(2020)"Performance assessment of a medium-scale turboprop engine designed for unmanned aerial vehicle(UAV)based on exergetic and sustainability metrics".Journal of Thermal Engineering 6(5): 697-711.

[18] Atilgan R.,Onder T.(2020)"Economy and exergy of aircraft turboprop engine at dynamic loads".Energy 213: 118827. https://doi.org/10.1016/j.energy.2020.118827.

[19] Dinc A.,Gharbia Y.(2022)"Exergy Analysis of a Turboprop Engine at Different Flight Altitude and Speeds Using Novel Consideration".International Journal of Turbo & Jet-Engines 39(4): 599-604. doi:10.1515/tjj-2020-0017.

[20] Dursun O.O., Toraman S.,Aygun H.(2022)"Modeling of performance and thermodynamic metrics of a conceptual turboprop engine by comparing different machine learning approaches".International Journal of Energy Research 46(15): 21084-21103. https://doi.org/10.1002/er.8484.

[21] Baklacioglu T., Turan O.,Aydin H.(2021)"Modeling of Relative Exergy Destruction for Turboprop Engine Components Using Deep Learning Artificial Neural Networks". 38(4): 377-390. doi:10.1515/tjj-2018-0047.

[22] Kirmizi M., Aygun H.,Turan O.(2023)"Performance and energy analysis of turboprop engine for air freighter aircraft with the aid of multiple regression".Energy 283: 129084. https://doi.org/10.1016/j.energy.2023.129084.

[23] Yuksel O.,Aygün H.(2025)"Comparative performance analysis of a turboprop engine used in regional aircraft by considering design and flight conditions".Aircraft Engineering and Aerospace Technology 97(3): 345-355. 10.1108/AEAT-07-2024-0194.